Dense Nonrigid Motion Tracking from a Sequence of Velocity Fields

François G. Meyer, R. Todd Constable, Albert J. Sinusas, and James. S. Duncan
Yale University School of Medicine, Department of Diagnostic Radiology
333 Cedar Street, P.O. Box 208042, New Haven, CT 06520-8042
e-mail: meyer@noodle.med.yale.edu

Abstract

We have addressed the problem of tracking the nonrigid motion of the heart using a sequence of velocity fields and a sequence of contours. The information from both the contours and the dense velocity fields is integrated into a deforming mesh that is placed over the myocardium at one time frame and then tracked over the entire cardiac cycle. The deformation is guided by a smoothing filter that provides a compromise between (i) believing the dense field velocity and the contour data when it is crisp and coherent in a local spatial and temporal sense and (ii) employing a temporally smooth cyclic model of cardiac motion when contour and velocity data are not trustworthy. The method has been carefully evaluated with simulated data and phantom data. Experiments with in vivo *data have also been conducted.*

1 Introduction

Many cardiac disorders manifest as abnormalities of myocardium function. The ability to accurately track the same region of interest and obtain noninvasive measurements of the regional contractility of the Left Ventricle (LV) of the heart is thus critical. The different methods that have addressed the problem of tracking nonrigid objects from a sequence of images can be classified into two broad groups. The first class is comprised of methods that exploit the correspondence between distinct features over time. Features can be points of highest curvature [1, 2], or landmarks obtained from MRI tagging [3, 4]. Correspondence between features is established over time, in order to recover the motion of the object from the sparse set of landmarks' trajectories. Unfortunately, without further information, the problem is underconstrained. The features' trajectories provide only a sparse sampling of the spatiotemporal trajectory of the object. This leads therefore to a classic assumption of the smoothness of motion. [5, 4, 6]. The second class of methods contains techniques that exploit time sequences of velocity fields. A sequence of velocity fields is estimated everywhere inside the object of interest [7, 8], and the goal is to recover the motion from the temporal sequence of snapshots of the velocity fields. The difficulty arise here from the fact that Eulerian (or spatial) velocity fields are measured with a large time step, and that we want to recover the Lagrangian path of each point in the object. In principle the integration of the Eulerian velocity should yield the path of each material point. In practice serious numerical difficulties arise. At a given instant the estimated position may not correspond to the true position of the material point, thus the velocity at this location will not coincide with the true velocity. When we integrate this velocity in order to estimate the position at the next instant, errors in the position will amplify. In addition the time step between two velocity fields is not controllable, and the integration can yield inaccurate results when the object is undergoing a large acceleration. Another problem stems from the fact that the velocity is only given on a discrete grid with limited resolution. Interpolation schemes are required to estimate velocities at positions not on the grid. Finally any noise in the velocity will be transmitted to the position estimates. This means that numerical errors in positions can grow rapidly in time as numerical integration proceeds. Very little work has been expended on the subject of nonrigid motion recovery of a complete object from a sequence of velocity fields. It is a difficult problem because it is nonlinear and unstable. However it is an important problem since there are many different ways to acquire velocity information: phase contrast MRI, Doppler ultrasound, optical flow, and others. The major contribution of this work is to explore and propose a completely new framework to track the entire LV from a sequence of velocity fields, and a sequence of contours.

2 Data acquisition

The tracking algorithm utilizes two temporal sequences of data: (i) a time sequence of 16 velocity fields (the heart cycle is divided into 16 instants) ; and

(ii) a time sequence of 16 contours of the LV: the endocardium (inner contour) and the epicardium (outer contour). The velocity maps and magnitude images are acquired over the heart cycle, using a technique, termed *phase contrast cine magnetic resonance imaging* (PC MRI) [9]. The technique combines phase contrast imaging methods, that can deliver quantitative measurement of motion [9], with cardiac cine techniques. We emphasize the case where velocity measurements are obtained by PC MRI, although we note that velocities can be directly estimated from the spatiotemporal changes of the intensity function [7, 8]. At any given instant we have access to the magnitude image of the PC MRI sequence, and we extract the contours of the myocardium using the deformable contour/region growing approach presented in [10].

3 Tracking algorithm

The geometry of the myocardium is characterized by a deforming mesh composed of N nodes $\xi_1, \ldots, \xi_N$. The partition is composed of quadrilaterals (see Fig. 5). Each quadrilateral has two nodes on the endocardium and two nodes on the epicardium. We assume that the kinematic state of the LV can be accurately characterized, at any instant, by a spatial piecewise polynomial approximation of the phase-contrast velocity field. This "spline-vector" approximation is uniquely characterized by a basis of N functions $\{\Phi_i\}_{i=1,\ldots,N}$ (one for each node) with local support. We assume that the support of the basis functions are moving along with the deformation of the domain. We thus have

$$\Phi_i(\mathbf{x}(\xi_i, k)) = 1 \qquad \forall k = 0, \ldots, T \tag{1}$$

where $\mathbf{x}(\xi_i, k)$ is the two-dimensional position of the node ξ_i at time k. Let $\mathbf{W}$ be the space spanned by the basis functions $\{\Phi_i\}$. Let $\mathbf{v} = (u, v)$ be the spatial velocity field at time k ; this velocity field is the k-th velocity fields generated by the MR acquisition sequence. We define $(u^\star, v^\star)$ as the spline-vector approximation of (u, v) over $\mathbf{W} \times \mathbf{W}$. $(u^\star, v^\star)$ can be expanded into the basis $\{\Phi_i\}$

$$u^\star(x) = \sum_{i=1}^{N} u_i^\star \Phi_i(x) \qquad v^\star(x) = \sum_{i=1}^{N} v_i^\star \Phi_i(x) \tag{2}$$

where $(u_i^\star, v_i^\star)$ is the nodal value of the velocity for the node ξ_i. For each node ξ_i we define a state vector, $\mathbf{s}_i$, that characterizes the "true" value of the node's kinematics. We will not be able to calculate directly $\mathbf{s}_i$, but we will derive *measurements* related to $\mathbf{s}_i$ at every instant k. For each node, we construct a measurement vector, $\mathbf{m}_i$, composed of two components: position, and velocity. The velocity component is the nodal value of the velocity $(u_i^\star, v_i^\star)$. The position component is derived from the contours of the LV at time k. The measurements are corrupted observations that are related to the "true" kinematics of the node. Our goal is to process the measurements $\{\mathbf{m}_i(0), \ldots \mathbf{m}_i(k), \quad i = 1, .., N\}$ in order to obtain the best estimate of $\{\mathbf{s}_i(k), \quad i = 1, .., N\}$, the kinematic state of the LV at time k. Assuming that the motion of the myocardium is governed by a set of differential equations, we can derive a model of the LV's dynamic behavior. We use a temporal smoothing filter that generates smooth estimates of $\mathbf{s}_i$, for each node ξ_i of the mesh. Formulating this problem as an estimation problem makes it possible to integrate position information and velocity information into a consistent framework.

3.1 Measurement definition

The velocity field $\mathbf{v} = (u, v)$ that we obtain at time k from the PC MRI sequence is composed of Eulerian velocities: $\mathbf{v}(\mathbf{x}, k)$ is the velocity of a material point that occupies the position $\mathbf{x}$, at time k ; however, we can not identify this material point. In order to build a kinematic measurement for each node ξ_i at time k, we need to calculate the Lagrangian velocity, $\mathbf{v}_i$, of the node, $\mathbf{v}_i(k) = \mathbf{v}(\mathbf{x}(\xi_i, k), k)$; where $\mathbf{x}(\xi_i, k)$ is the two-dimensional position of the node at time k. To achieve this, we first match the LV geometry (defined by the contours of the LV) at time k. with a prediction of the mesh geometry, generated by the tracking algorithm (see Fig 1). Each node of the predicted mesh is projected onto the extracted contours (see Fig 1). This defines the position measurement for this node, at the current instant. Ideally this measurement should correspond to an estimate of the position of the material point ξ_i. We now have a measurement $(\tilde{x}_i, \tilde{y}_i)$ of the two-dimensional position $\mathbf{x}(\xi_i, k)$ of each node ξ_i at time k. Using the mesh defined by the projected nodes, we then calculate the nodal value of the velocity $(u_i^\star, v_i^\star)$ at each node (see Fig 1) with a vector spline approximation method. Inside each quadrilateral of the mesh, a bilinear model of the velocity describes the transmural variation of the velocity across the wall. The limited transmural resolution of the data makes it difficult to fit higher order models. At this point we can construct a measurement vector $\mathbf{m}_i$ for each node ξ_i. The equations of $\mathbf{m}_i$ for one component, x for instance, (similar relations can be derived for y), is given by

$$\mathbf{m}_i = \begin{bmatrix} \tilde{x}_i \\ u_i^\star \end{bmatrix} \tag{3}$$

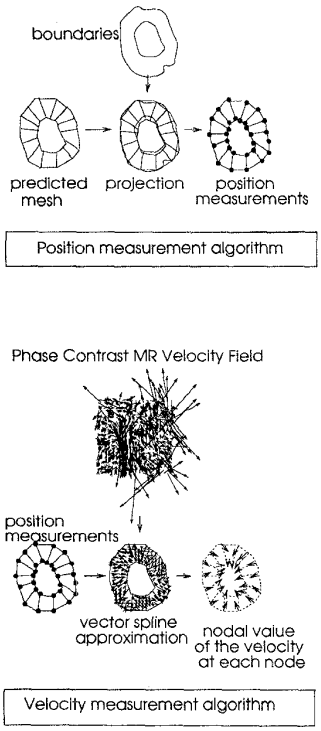

Figure 1: Top: position measurement, Bottom: velocity measurement. The position measurement is used as an input for the velocity measurement algorithm.

where $(u_i^\star, v_i^\star)$ is the nodal value of the velocity, and $\tilde{x}_i$ is position measurement.

3.2 Dynamic behavior of the mesh

In this work, we assume the motion of the heart is periodic, and we expand the trajectory of each node ξ_i into a basis of sine functions. Due to the problem of limited temporal resolution (16 time samples only are available at the moment), high order terms tend to be difficult to estimate. We only retain the first two terms of the expansion. For the clarity of the presentation and to lighten the notation, from now on we drop the index i of the node ξ_i wherever it can be done without causing confusion. A continuous model of the trajectory $\mathbf{x}(k) = \mathbf{x}(\xi, k)$ of the node ξ, is

$$\mathbf{x}(t) = \bar{\mathbf{x}} + A\sin(2\pi\omega t + \varphi) \qquad t \in \mathbb{R} \qquad (4)$$

where t is the continuous time index, $\bar{\mathbf{x}}$ is the mean position over the period, and A is the amplitude of the motion. The frequency of the oscillator is $2\pi\omega = 2\pi/T$ where T is the period of the heart cycle. This system model is only valid over a short time interval. Nevertheless, as opposed to the constant-velocity, or constant-acceleration models, (4) explicitly models the trajectory as being closed. Finally, we also add some noise in the model (4) to accommodate significant differences between (4) and the real motion of the myocardium. Let $\mathbf{s}(k)$ be be the state vector that describes one component (x for instance) of the state of the node ξ, $\mathbf{s}(k) = [\bar{x}, x, \dot{x}]^T(k)$. From (4) we derive the following linear dynamic system that characterizes the discrete time evolution of $\mathbf{s}(k)$:

$$\mathbf{s}(k+1) = \mathbf{F}\,\mathbf{s}(k) + \boldsymbol{\zeta}(k) \qquad (5)$$

with

$$\mathbf{F} = \begin{bmatrix} 1 & 0 & 0 \\ 1-\cos(\omega\Delta t) & \cos(\omega\Delta t) & \frac{1}{\omega}\sin(\omega\Delta t) \\ \omega\sin(\omega\Delta t) & -\omega\sin(\omega\Delta t) & \cos(\omega\Delta t) \end{bmatrix}$$

where $\boldsymbol{\zeta}(k) = [\zeta_1, \zeta_2, \zeta_3]^T(k)$ is a zero mean Gaussian noise of covariance matrix $\mathbf{Q}(k)$; and where Δt is the time interval between two time samples. With our definition of the state vector, and from (3) the measurement system takes the form

$$\mathbf{m}(k) = \mathbf{H}\mathbf{s}(k) + \boldsymbol{\eta}(k) \quad \text{with} \quad \mathbf{H} = \begin{bmatrix} 0 & 1 & 0 \\ 0 & 0 & 1 \end{bmatrix} \qquad (6)$$

where $\boldsymbol{\eta} = [\eta_1, \eta_2]^T(k)$ is a zero mean Gaussian noise vector of covariance matrix $\mathbf{R}(k)$. The problem is then the following: Given the observations : $\mathbf{m}(0), \ldots, \mathbf{m}(T)$, we wish to obtain an optimal estimate of the state vector $\mathbf{s}$ at any given time k within the interval, $\mathbf{s}(k|k)$, that minimizes the mean-norm-squared-error. There exists an efficient recursive algorithm to calculate this estimate: the fixed interval smoothing filter [11].

3.3 Optimal temporal smoothing

The optimal linear smoother is a combination of two optimum linear filters: a forward filter, and a backward filter. The forward filter processes the data from time 0 to some time k within the interval, and generates the optimal estimate $\hat{\mathbf{s}}_f(k|0,k)$ as well as $\mathbf{P}_f(k|0,k)$, the covariance matrix of $\hat{\mathbf{s}}_f(k|0,k)$. Similarly, the backward filter generates $\hat{\mathbf{s}}_b(k|k+1,T)$, the optimal estimate at time k based upon all the measurements from time $k+1$ to time T as well as $\mathbf{P}_b(k|k+1,T)$, the covariance matrix of $\hat{\mathbf{s}}_b(k|k+1,T)$. The smoothed estimate $\hat{\mathbf{s}}_s(k)$, based upon all the measurements from time 0 to time T, is generated by optimally combining the value of the forward filter and the value of the backward filter at time k [11] :

$$\hat{\mathbf{s}}_s(k) = \mathbf{P}_s^{-1}(k)\left[\mathbf{P}_f^{-1}(k|0,k)\hat{\mathbf{s}}_f(k|0,k) + \mathbf{P}_b^{-1}(k|k+1,T)\hat{\mathbf{s}}_b(k|k+1,T)\right] \qquad (7)$$

where $\mathbf{P}_s(k)$, the covariance matrix of $\hat{\mathbf{s}}_s(k)$, is

$$\mathbf{P}_s^{-1}(k) = \mathbf{P}_f^{-1}(k|0,k) + \mathbf{P}_b^{-1}(k|k+1,T) \quad (8)$$

The optimal forward estimate $\hat{\mathbf{s}}_f(k+1|0,k+1)$ is generated by filtering data prior to time k with a Kalman filter [12]. The discrete-time system (5) propagates forward in time. In order to build the backward estimate, it is useful to consider time running backward. It is possible to build a process equivalent to (5) up to second order properties, but with state model propagating in reverse time [11]:

$$\mathbf{s}_b(k) = \mathbf{F}_b(k+1)\mathbf{s}_b(k+1) + \boldsymbol{\zeta}_b(k+1) \quad (9)$$

where $\boldsymbol{\zeta}_b(k)$ is a zero mean Gaussian noise of covariance matrix $\mathbf{Q}_b(k)$. $\mathbf{F}_b(k)$ and $\mathbf{Q}_b(k)$ are given by

$$\begin{aligned} \mathbf{F}_b(k+1) &= \mathbf{F}^{-1}(k)\left[I - \mathbf{Q}(k)\boldsymbol{\Pi}^{-1}(k+1)\right] \\ \mathbf{Q}_b(k+1) &= \mathbf{F}_b(k+1)\mathbf{Q}(k)\mathbf{F}_b^T(k+1) \end{aligned}$$

where $\boldsymbol{\Pi}(k)$ is the covariance matrix of $\mathbf{s}$ at time k. Kalman filtering can then be used on the system (9) to generate the optimal estimate of $\mathbf{s}(k)$ given measurements from time $k+1$ to time T. We model $\mathbf{R}(k)$ as a diagonal matrix. The first term on the diagonal is the variance of the position measurement, and it is proportional to the inverse of the magnitude of the gradient of the magnitude signal. The second term on the diagonal of $\mathbf{R}(k)$ is the variance of the velocity, and at the moment we use a fixed uniform variance for any velocity measurement inside the myocardium. We model $\mathbf{Q}(k)$ as a diagonal matrix. The values of $\mathbf{Q}(k)$ can be adjusted to obtain different levels of temporal smoothing. There is a bootstrapping mode to initialize the filter: it requires two time step to get an estimate of the acceleration (or equivalently an estimate of the mean position).

4 Experiments

4.1 Numerical simulations

A quantitative evaluation of the method has been performed using numerical simulations of velocities and contour data, that are representative of the motion of the myocardium in a general way. We present here the result of one experiment where a 2-D annulus undergoes a periodic expansion and translation. The trajectory of the center of the annulus is a circle:

$$\begin{aligned} x_c &= x_0 + \Delta_c \cos(\omega t) \\ y_c &= y_0 + \Delta_c \sin(\omega t) \end{aligned}$$

with $\Delta_c = 2.5 pixels$. The internal radius $\rho(k)$ is evolving according to

$$\rho(k) = \rho(0) + \lambda(\rho(0)) \sin(\omega t)\Delta\rho$$

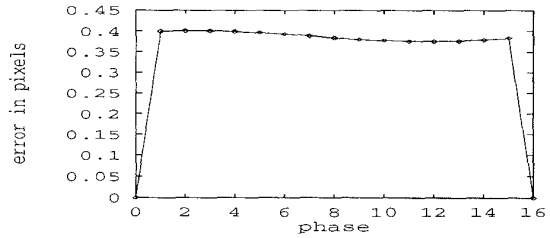

Figure 2: Expanding and translating annulus: RMS tracking error at each instant k. The average was taken over all nodes.

with $\lambda(\rho(0)) = (\rho_{out} - \rho(0))/(\rho_{out} - \rho_{in})$, and $\omega = 2\pi\frac{100}{60}$, $\rho_{out} = 40\ pixels$, $\rho_{in} = 14\ pixels$, $\Delta_\rho = 2.5\ pixels$, with an effective heart rate of 100 $beats/min$. 16 images were simulated over one heart cycle. The motion of the annulus was tracked using 16 nodes on the inner contour and 16 nodes on the outer contour. For this experiment the velocity components were coded as integers, and therefore truncations errors resulted in noise on the velocity fields. The position of the tracked nodes have been compared to the theoretical values (determined analytically). Two different errors were calculated:
(1) a root mean squared (RMS) error over all nodes, at each instant k

$$\text{RMS error}(k) = \sqrt{\frac{1}{N}\sum_{i=1}^{N} \|\mathbf{x}_i(k) - \hat{\mathbf{x}}_i(k)\|^2} \quad (10)$$

where $\mathbf{x}_i(k)$ is the true position of the node ξ_i, and $\hat{\mathbf{x}}_i(k)$ is the result of the tracking ;
(2) a relative error over the total path length, for each node i

$$\text{relative error}(i) = \frac{\sqrt{\frac{1}{T}\sum_{k=0}^{T} \|\mathbf{x}_i(k) - \hat{\mathbf{x}}_i(k)\|^2}}{\int_0^T d\mathbf{x}_i} \quad (11)$$

where $\int_0^T d\mathbf{x}_i$ is the total path length of the node i. The mean relative error over all the nodes was then calculated. Figure 2 shows the RMS error, in pixels, for any phase over the heart cycle. The estimate build at the second time step (time 1) is calculated using the bootstrapping mode, and thus relies only on the noisy velocity measured at time 0. Consequently, the position estimate at time 1 does not coincide with the true position. As a result, the rest of the path is globally translated from the theoretical trajectory, and this systematic error creates a small RMS error. The mean relative error over all the nodes was 1.8% of the total path length. Given the magnitude of the motion, the agreement between the measured data and the theoretical values is good.

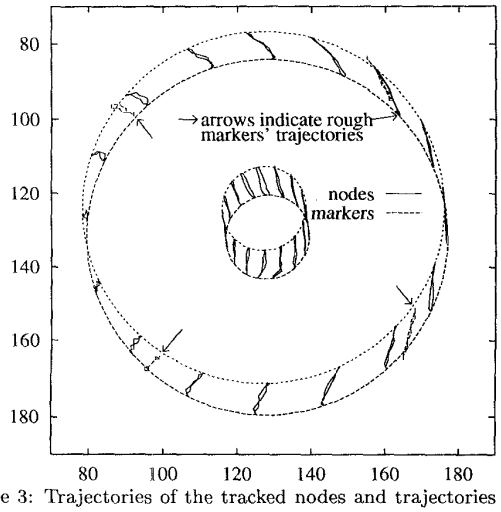

Figure 3: Trajectories of the tracked nodes and trajectories of the hand-traced markers. The contours of the phantom are superimposed at time 4 and at time 12 only.

4.2 Phantom study

The phantom consisted of a gel-filled disk undergoing rotation and translation in the plane. The maximum translation was $1cm$, and the maximum rotation was 20^o. The motion of the phantom was periodic with an effective heart rate of $66beats/min$. The phantom was imaged in a quadrature head coil using a cine PC gradient echo imaging sequence. The disk had four small markers on its outer edge. The trajectories of the markers have been manually hand traced, and using triangulation, the theoretical position of any point inside the phantom could be calculated at any instant. We put 16 nodes on the inner contour and 16 nodes on the outer contour. The trajectories of the nodes, and the trajectories of the markers are shown in Fig. 3. The contours of the phantom at time 4 and at time 12 are also shown. RMS errors in the position of the nodes using the proposed approach have been calculated at each instant, and are shown in Fig. 4. The mean relative error over all the nodes was 4.4% of the total path length. Given the initial error on the theoretical positions of the nodes, the calculated positions are in good agreement with the true values.

4.3 *In Vivo* Data

To further validate our approach the tracking algorithm has been tested *in vivo* with an open chest canine model of infarction. A dog was positioned in a quadrature head coil for MR imaging using the cine PC gradient echo sequence. Velocity maps were acquired both before and one hour after a permanent occlusion of the proximal left anterior descending artery (LAD). We recognize that the motion of the myocardium is three-dimensional. We consider here a simplified 2-D version of the problem. The LV has been tracked before the coronary occlusion with a partition consisting of 24 nodes on the endocardium and 24 nodes on the epicardium. The tracking started at time 0 (end diastole) when the wall was the thinnest ; and the nodes were initially equally sampled along each contour. Figure 5 shows on the left the deformed partition at four instants through the cardiac cycle. The fitted spline vector field is shown on the right in Fig. 5 at the corresponding instants. After occlusion of the LAD the LV has been tracked with a similar partition and the same number of nodes.

5 Conclusion

We have addressed the problem of the recovery of nonrigid motion from a sequence of velocity fields. We have proposed a new unified framework that exploits velocity fields and contour information to track the nonrigid motion of the LV. The method has been carefully evaluated with simulated data and phantom data. Thus, our unified framework for assessment of nonrigid myocardial motion, which integrates contour information with PC velocity maps provides a reliable estimate of 2-D motion. This approach is being extended to 3-D.

Acknowledgments

This work is supported in part by NIH Grant R01HL44803 from the National Heart, Lung and Blood Institute, by United States Air Force Grant F49620-93-1-0575. The authors thank Amit Chakraborty for his help with the extraction of the contours of the LV, and Matthew Robson for his help in the design of the synthetic annulus sequence.

References

[1] J.S. Duncan, R.L. Owen, L.H. Staib, and P. Anandan. Measurement of non-rigid motion using contour shape descriptors. In *Proc. Conference Computer Vision and Pattern Recognition, Hawaii*, pages 318–324, June 1991.

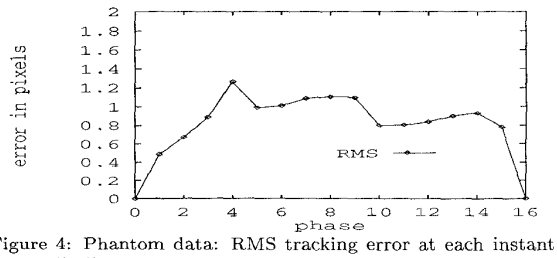

Figure 4: Phantom data: RMS tracking error at each instant k, in solid line.

[2] P. Shi, A. Amini, G. Robinson, A. Sinusas, R.T. Constable, and J. Duncan. Shape-based 4-D left ventricular myocardial function analysis. In *Proc. IEEE Workshop on Biomedical Image Analysis, Seattle, Washington*, pages 88–97, 1994.

[3] T.S. Denney and J.L. Prince. Reconstruction of 3-D left ventricular motion from plannar tagged cardiac MR images: An estimation approach. *IEEE Trans. on Medical Imaging*, pages 625–635, Dec. 1995.

[4] A.A. Young, D.L. Kraitchman, L. Dougherty, and L. Axel. Tracking and finite element analysis of stripe deformation in magnetic resonance tagging. *IEEE Trans. on Medical Imaging*, pages 413–421, Sept. 1995.

[5] A. Pentland and B. Horowitz. Recovery of nonrigid motion and structure. *IEEE Trans. on Pattern Analysis and Machine Intelligence*, pages pp 730–742, July 1991.

[6] D. Metaxas and D. Terzopoulos. Shape and nonrigid motion estimation through physic-based synthesis. *IEEE Trans. on Pattern Analysis and Machine Intelligence*, pages 580–591, June 1993.

[7] J.L. Prince and E.R. McVeigh. Motion estimation from tagged MR image sequences. *IEEE Trans. on Medical Imaging*, pages 238–249, June 1992.

[8] S.M. Song, R.M. Leahy, D.P. Boyd, B.H. Brundage, and S. Napel. Determining cardiac velocity fields and intraventicular pressure distribution from a sequence of ultrafast CT cardiac images. *IEEE Trans. on Medical Imaging*, 13:2:386–397, 1994.

[9] N.J. Pelc, R.J. Herfkens, A. Shimakawa, and D. Enzmann. Phase contrast cine magnetic resonance imaging. *Magnetic Resonance Quaterly*, Vol.7, No 4:229–254, 1991.

[10] A. Chakraborty, L.H. Staib, and J.S. Duncan. Deformable boundary finding influenced by region homogeneity. In *Proc. of CVPR'94, Seattle, Washington*, pages 624–627, 1994.

[11] G.S. Sidhu and U.B. Desai. New smoothing algorithms based on reversed-time lumped models. *IEEE Trans. on Automat. and Contr.*, Vol.21, no.4:538–541, Aug. 1976.

[12] P.S.Maybeck. *Stochastic Models, Estimation and Control, Volumes 1 & 2.* Academic Press, 1982.

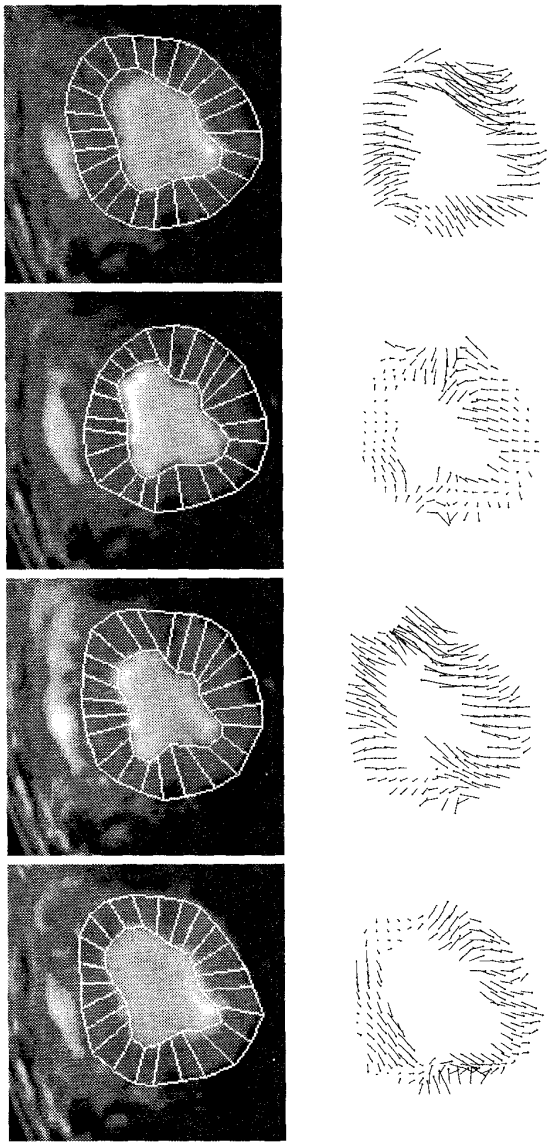

Figure 5: *in vivo* study, pre-infarct. Left: results of the tracking at time 1, 5, 9, and 14. Right: vector spline approximation of the velocity field at time 1, 5, 9, and 14. The tracking started at time 0 (end diastole)